Absorption and Emission Cross Section of Er^{3+} Doped Silica fibers

William L. Barnes
Richard I. Laming
Eleanor J. Tarbox
P. R. Morkel

Reprinted from
IEEE JOURNAL OF QUANTUM ELECTRONICS
Vol. 27, No. 4, April 1991

Absorption and Emission Cross Section of Er^{3+} Doped Silica Fibers

William L. Barnes, Richard I. Laming, Eleanor J. Tarbox, and P. R. Morkel

Abstract—**A detailed set of measurements is presented on determining the emission and absorption cross sections of Er^{3+} doped fibers for the $^4I_{13/2} \rightarrow {}^4I_{15/2}$ transition. Two techniques are employed: the Fuchtbauer–Ladenberg analysis, based on spectroscopic data; and a more direct technique involving optical saturation of the transition. The cross sections, and in particular their ratio, are significantly different for the two techniques. Possible reasons for this are discussed, and we conclude that the Fuchtbauer–Ladenberg approach is inappropriate in this situation.**

Introduction

ERBIUM doped optical fiber amplifiers have been well characterized experimentally, and practical systems have been demonstrated [1]–[3]. Considerable emphasis is therefore placed on performance optimization using numerical modeling. For these models to be relevant, it is important to establish material parameters accurately. Precise measurement of the optical absorption and fluorescence cross sections of the doped fiber is particularly important. This paper is concerned with the determination of these parameters.

Cross sections are commonly derived from experimental values of fluorescence and absorption bandwidths [4]–[7]. This is done using the Fuchtbauer–Ladenberg equation, which may be derived from the Einstein relations. Performing such an analysis, we find that $\sigma_E \sim 1.2\sigma_A$, in broad agreement with other workers. While such results are widely accepted, they do not agree with the results of simple gain measurements. We have noted that a length of doped fiber that shows an unpumped loss of, say, 10 dB, never shows a gain of 10 dB, even under extreme pumping. Since the ratio of maximum available gain to the unpumped loss should be the same as the ratio of the cross sections, the Fuchtbauer–Ladenberg approach looks flawed.

An independent measure of the cross sections is required. We have chosen to do this by measuring the saturation power, i.e., the pump power required to cause a 50% inversion in the metastable level. Three fiber types are analyzed, differing in core composition. The work reported is divided into the following three parts.

Manuscript received November 5, 1990. This work was supported in part by the Amoco Technology Company and Pirelli General.

W. L. Barnes, R. I. Laming, and P. R. Morkel are with the Optical Fibre Group, University of Southampton, Southampton SO9 5NH, England.

E. J. Tarbox is with Pirelli General, Eastleigh, Southampton, England.

IEEE Log Number 9144328.

1) *Fuchtbauer–Ladenberg analysis*: to enable comparison of this work to that of others.

2) *Gain–loss measurements*: to determine the ratio of the peak absorption to peak emission cross section directly.

3) *Saturation power measurements*: to independently determine the absorption cross section and, thus, with the aid of gain–loss measurement, the emission cross section.

Fuchtbauer–Landenberg Analysis

The emission and absorption cross sections may be related to the fluorescence and absorption bandwidths, provided the spontaneous lifetime and level degeneracy are also known. The Fuchtbauer–Ladenberg equations are derived from the Einstein relations for the A and B coefficients of a two-level system (see the Appendix). The cross sections may be written as follows:
for emission,

$$\sigma_{21} = \frac{\lambda^2}{8\pi\mu^2} A_{21} g(\nu) \tag{1}$$

and for absorption,

$$\sigma_{12} = \frac{g_2}{g_1} \frac{\lambda^2}{8\pi\mu^2} A_{21} g'(\nu). \tag{2}$$

The wavelength of peak emission–absorption is λ, while the line shape for emission is $g(\nu)$ and $g'(\nu)$ for absorption. The spontaneous decay rate, A_{21} is given by $1/\tau_{\text{spont}}$ which, provided there is no nonradiative decay, is equal to the inverse fluorescence lifetime $1/\tau_{fl}$. (This point will be discussed later.) The refractive index is μ and the level degeneracies are g_1 and g_2.

Since the line shape is in general not simple, the effective linewidth $\Delta\lambda_{\text{eff}}$ is defined through the relation

$$I_{pk} \Delta\lambda_{\text{eff}} = \int_0^\infty I(\lambda)\, d\lambda. \tag{3}$$

The line shape function may be written as

$$g(\nu) = \frac{I_{pk}}{\int I\, d\nu} \tag{4}$$

so that

$$g(\nu) = \frac{\lambda^2}{c} \frac{1}{\Delta\lambda_{\text{eff}}}. \tag{5}$$

The Fuchtbauer-Ladenberg equations (1) and (2) may now be rewritten as

$$\sigma_{21} = \frac{\lambda^4}{8\pi\mu^2 c} \frac{1}{\tau_{fl}\Delta\lambda_E} \tag{6}$$

and

$$\sigma_{12} = \frac{g_2}{g_1} \frac{\lambda^4}{8\pi\mu^2 c} \frac{1}{\tau_{fl}\Delta\lambda_A}. \tag{7}$$

Thus, the ratio of absorption to emission cross section is given by

$$\frac{\sigma_{12}}{\sigma_{21}} = \frac{g_2}{g_1} \frac{\Delta\lambda_E}{\Delta\lambda_A}. \tag{8}$$

The level degeneracy is easily determined from the angular quantum number J as $2J + 1$. Thus, for the $^4I_{13/2}$ (upper) level, the degeneracy is 7; and for the $^4I_{15/2}$ (lower) level, it is 8, In silica, the degeneracy is lifted by the local electric field [8] Stark splitting, so that the bandwidths that we measure already have the effect of degeneracy built into them. Equation (8) thus becomes

$$\frac{\sigma_{12}}{\sigma_{21}} = \frac{\Delta\lambda_E}{\Delta\lambda_A}. \tag{8a}$$

The fluorescence lifetimes of a large number of fibers were measured, and all were found to display exponential decay. The maximum concentration of erbium in the GeO_2–SiO_2 glass was $\sim 1 \times 10^{25}$ ions/m^3, and in the Al_2O_3–SiO_2-type glass it was $\sim 7 \times 10^{25}$ ions/m^3, thus avoiding problems associated with concentration quenching and clustering. Short lengths of fiber were pumped at ~ 800 nm, the length being kept short enough (typically < 0.2 dB of loss at 1.5 μm) to avoid amplified spontaneous emission (ASE). We found the fluorescent decay times to be

GeO_2–SiO_2 $\quad 12.1 \pm 0.3$ $\quad$ ms

Al_2O_3–SiO_2 $\quad 10.2 \pm 0.3$ $\quad$ ms.

(The only GeO_2–Al_2O_3–SiO_2 fiber measured had the same lifetime as the Al_2O_3–SiO_2 fiber.)

Care was taken in obtaining fluorescence data to take account of the spectral response of the measurement system. Absorption data were recorded using a cutback technique. While making these measurements, the 980 nm absorption band was also examined. Attenuation data show that a considerable amount of water (OH^-) remains in the fibers (Fig. 1). (The water peak was removed from the data before calculating the linewidths.) The emission and absorption linewidths ($\Delta\lambda$) may be calculated by rearranging (3) as

$$\Delta\lambda = \frac{1}{I_{pk}} \int_0^\infty I(\lambda)\, d\lambda \tag{9}$$

where $I_{\lambda pk}$ is the intensity at the peak of the emission or absorption plot. Table I shows the linewidths. The cross-section ratios σ_E/σ_A are shown in Table II.

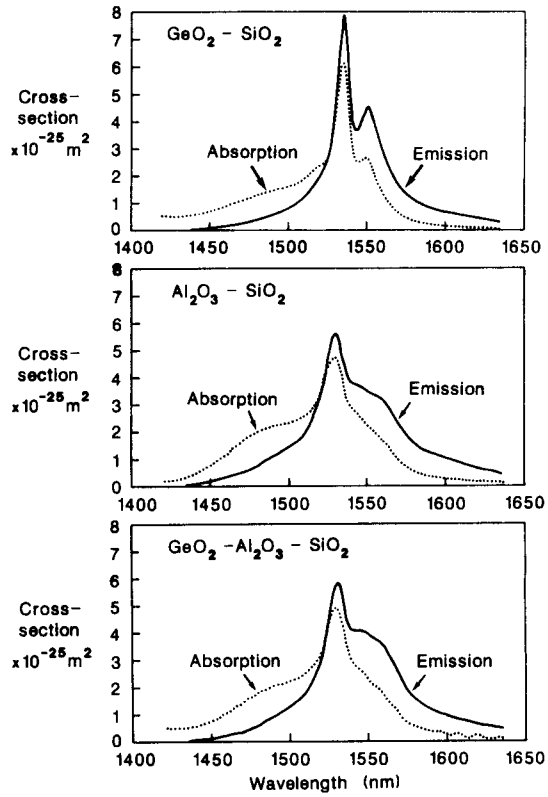

Fig. 1. Spectral variation of the emission and absorption cross section derived using the Fuchtbauer-Ladenberg approach.

TABLE I
MEASURED FLUORESCENT AND ABSORPTION BANDWIDTHS

Fiber Type	Fluorescence Linewidth (nm)	Absorption Linewidth (nm)
GeO_2–SiO_2	36^{+1}_{-1}	46^{+3}_{-2}
Al_2O_3–SiO_2	60^{+3}_{-2}	72^{+4}_{-3}
GeO_2–Al_2O_3–SiO_2	58^{+3}_{-2}	68^{+4}_{-3}

TABLE II
CROSS-SECTION RATIO σ_E/σ_a AS DERIVED SPECTROSCOPICALLY

Fiber Type	σ_E/σ_A
GeO_2–SiO_2	1.28 ± 0.13
Al_2O_3–SiO_2	1.20 ± 0.11
GeO_2–Al_2O_3–SiO_2	1.17 ± 0.10

TABLE III
EMISSION AND ABSORPTION CROSS SECTIONS, AS DERIVED USING THE FUCHTBAUER-LADENBERG METHOD

GeO_2–SiO_2	$7.9^{+0.8}_{-0.5}$	$6.2^{+0.6}_{-0.3}$
Al_2O_3–SiO_2	$5.6^{+0.3}_{-0.2}$	$4.7^{+0.3}_{-0.2}$
GeO_2–Al_2O_3–SiO_2	$5.8^{+0.3}_{-0.2}$	$4.9^{+0.3}_{-0.2}$

With the information in Table II, we can compute the relevant cross sections. We show them in Table III. The resulting spectral cross-section data are shown in Fig,. 1(a)–(c).

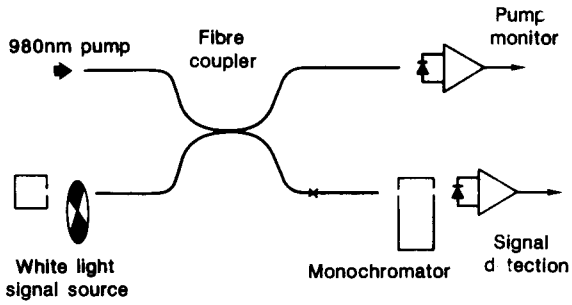

Fig. 2. Experimental arrangement for recording gain-loss data.

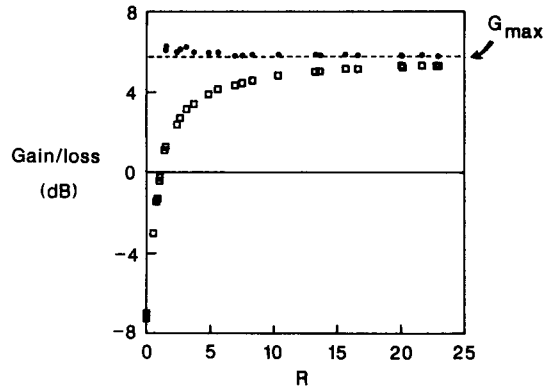

Fig. 3. Sample gain-loss data for the GeO_2–SiO_2 fiber. Gain is plotted as a function of pump power. Also shown is the predicted value of G_{max}, based on (14).

Gain-Loss Measurements

The ratio of gain to loss of a length of doped fiber was measured as a function of pump power using the arrangement shown in Fig. 2. A $Ti^{3+}:Al_2O_3$ laser was used as the pump source, operating at 980 nm for the GeO_2–SiO_2 fiber and 978 nm for the other two types. As the pump power is increased, the output at the signal wavelength rises asymtotically toward an upper limit. Experimental data for the GeO_2–SiO_2 fiber type is shown in Fig. 3. It was not possible to get closer than ~10% of the asymptotic limit with the available pump power, particularly for fibers containing Al_2O_3. As a result, the data must be extrapolated in some way.

If we neglect the radial variations of both the dopant distribution and the optical fields, and also ignore variations along the length of the fiber, then the single pass gain G may be given by

$$G = \exp\left[n_T \cdot l \frac{W_{13}\sigma_E - \sigma_A/\tau}{W_{13} + 1/\tau}\right] \tag{10}$$

where W_{13} is the pump rate, τ is the radiative lifetime, and n_T is the number density of ions in the sample. (These assumptions are justified for high pump powers, and short lengths of low doped fibers.) The pump rate is directly proportional to the pump power P. In the bleached condition, i.e., no gain or loss, the pump rate is equal to $\sigma_A/\tau\sigma_E$, and the pump power to achieve this is P_{th}. Equation (10) can thus be rewritten as

TABLE IV
Ratio of Gain to Loss for the Three Fibre Types

Fiber Type	σ_E/σ_A
GeO_2–SiO_2	0.84 ± 0.03
Al_2O_3–SiO_2	0.82 ± 0.05
GeO_2–Al_2O_3–SiO_2	0.94 ± 0.09

$$G = \exp\left[n_T l\sigma_E \frac{P - P_{th}}{P + P_{th}\dfrac{\sigma_E}{\sigma_A}}\right] \tag{11}$$

putting $R = P/P_{th}$, (11) becomes

$$G = \exp\left[n_T l\sigma_E \left(\frac{R-1}{R + \dfrac{\sigma_E}{\sigma_A}1}\right)\right] \tag{12}$$

or, setting $n_T \cdot l\sigma_E$ to G_{max}, we have

$$G = \exp\left[\left(\frac{R-1}{R + \dfrac{\sigma_E}{\sigma_A}}\right) G_{max}\right]; \tag{13}$$

reexpressing the gain in decibels, we then have

$$G = G_{max}\left(\frac{R-1}{R + \dfrac{\sigma_E}{\sigma_A}}\right). \tag{14}$$

Initially, σ_E/σ_A is set to 1. G_{max} may then be predicted from the experimental data using (14). The ratio of G_{max} to L_{max} (the loss of the fiber when not pumped) provides a new value for σ_E/σ_A, which is then put into (14), and the experimental data are refitted. This process is repeated in a self-consistent way to obtain σ_E/σ_A. Equation (14) is an approximate expression in the present situation, however, the accuracy improves as R increases. This is seen in Fig. 3 where the predicted value of G_{max} soon converges to a fixed value. (Data were obtained for different fiber lengths, all having an unpumped loss ≤ 6 dB. With this condition, the ratio of gain to loss was found to be independent of length.) Analyzing our data in this way, we find the ratio of gain to loss to be as shown in Table IV.

Note that the considerable difference between Tables II and IV. (Note also that the ratio for the GeO_2–Al_2O_3–SiO_2 fiber type is considerably higher than the other two. Since the error in this measurement is greater than for the other two fiber types, the difference in ratios might not be too significant. The increased error arose from the considerable variation obtained on repeating the measurement several times, and was not ascribed to the error in a single set of data.)

Saturation Power Measurements

The fluorescent output power is directly proportional to the population n_2 of the metastable level and, for an infin-

itesimal section of fiber, this may be written as

$$n_2 = \frac{W_{13} n_T}{W_{13} + 1/\tau}. \tag{15}$$

To reach half the maximum value of the fluorescence, i.e., to get to an inversion of $n_t/2$, the pumping rate is given by

$$W_{13} = \frac{1}{\tau}. \tag{16}$$

In general, the stimulated rate between two levels i and j is given by

$$W_{ij} = \frac{\sigma_{ij} P_{ij}}{h\nu_{ij} A}. \tag{17}$$

Here σ_{ij} is the cross section of the transition, P_{ij} is the optical powr, $h\nu_{ij}$ is the photon energy, and A is the area of the infinitesimal segment. The pump power required to reach half inversion (i.e., bleach the transition) is called the saturation power and is given by

$$P_s = \frac{h\nu_{13} A}{\sigma_{13} \tau}. \tag{18}$$

The fluorescent power from the side of a short length of fiber was recorded as a function of pump power. The output increases asymtotically to some upper limit corresponding to full population inversion. An example of such data is shown in Fig. 4. From this, the saturation power and thus pump absorption cross section may be calculated via (18). Again we assume no nonradiative decay so that τ can be replaced by τ_{fl}. Knowing the absorption cross section at the pump wavelength, and knowing the spectral attenuation of both the 0.98 μm and 1.5 μm bands, the absorption cross section at ~ 1.53 μm may be calculated.

Of course, in the fiber, the situation is more complicated, so the radial distribution of pump field and dopant must be taken into account. In this case, the population inversion (and hence fluorescent intensity) is given by

$$n_2 = 2\pi \int_0^\infty \frac{W_{13}(r) n_T(r)}{W_{13}(r) + 1/\tau} \cdot r \cdot dr. \tag{19}$$

Such a calculation requires a knowledge of the dopant distribution $n_T(r)$. These were obtained by X-ray microprobe analysis of the preforms by the materials characterization service, Harwell, U.K. The data are shown in Fig. 5. Also recorded was the distribution of the index raising materials—Ge and Al. Data from the latter was used to generate an equivalent step index (ESI) [9], thus fixing the core radius with respect to the dopant distribution. In the case of the fiber, the numerical aperture, cutoff wavelength, and spot size can be used to predict the core radius using the Marcuse relation. Spot sizes were measured by a far-field scanning technique, and analyzed using the Petermann II definition of spot size [10], at pump and signal wavelengths. Using the above information, the experimental saturation curves (e.g., Fig. 4) were fitted using (19) to give pump absorption cross section; we found them to as shown in Table V.

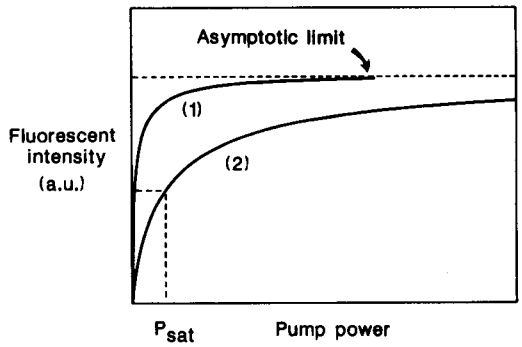

Fig. 4. Sample fluorescence saturation data. Fluorescent power is recorded as a function of pump power. Curve 2 is as 1, except that the x axis has been expanded by a factor of 10. Also shown is the asymptotic limit obtained using (15).

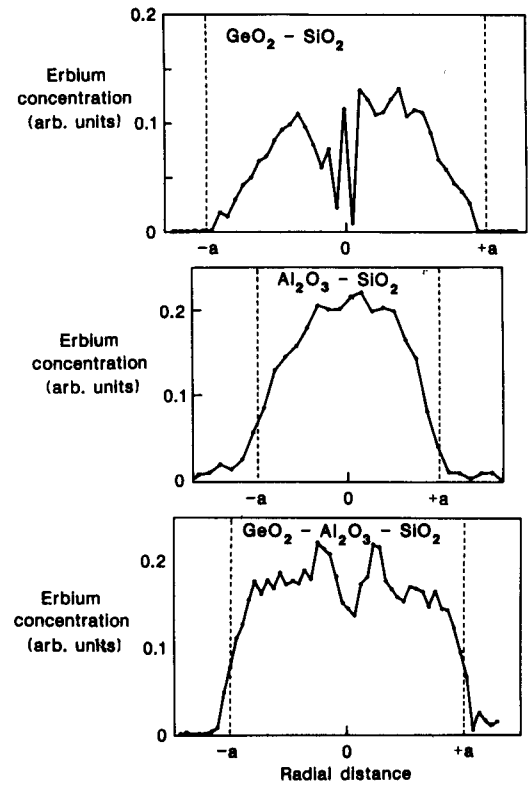

Fig. 5. Er^{3+} distribution for the three fibre types. The parameter a is the core radius as defined by the effective step index measurement—see text.

TABLE V
PUMP ABSORPTION CROSS SECTIONS

Fiber Type	980 nm Pump Cross Section $\times 10^{-25}$ m^2
GeO_2-SiO_2	2.52 ± 0.03
Al_2O_3-SiO_2	1.9 ± 0.3
GeO_2-Al_2O_3-SiO_2	1.7 ± 0.3

Knowing the ratio of absorption strengths for the two bands—as measured from the fiber—and the degree of overlap at each wavelength, the absorption cross sections

TABLE VI
EMISSION AND ABSORPTION CROSS SECTIONS AS DERIVED BY THE SATURATION METHOD

Fiber Type	Emission Cross Section $\times 10^{-25}$ m^2	Absorption Cross Section $\times 10^{-25}$ m^2
GeO_2-SiO_2	6.7 ± 0.3	7.9 ± 0.2
Al_2O_3-SiO_2	4.4 ± 0.6	5.1 ± 0.6
GeO_2-Al_2O_3-SiO_2	4.4 ± 1.0	4.7 ± 0.8

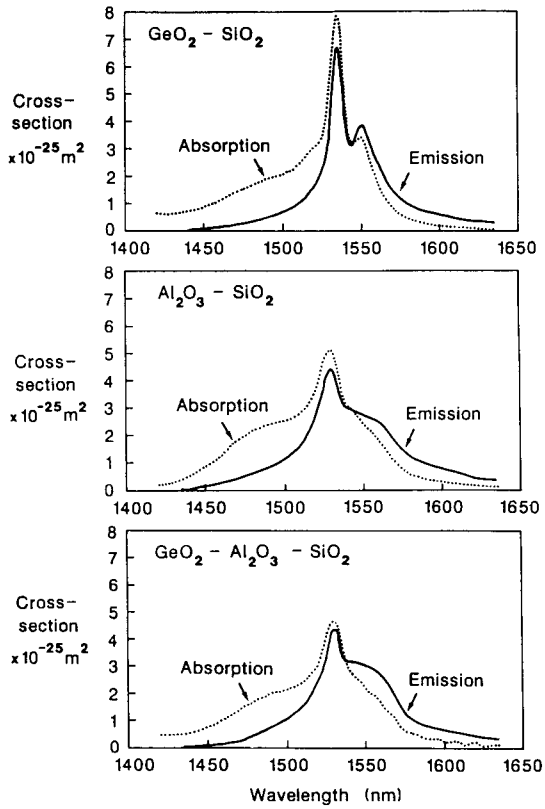

Fig. 6. Cross-section data as derived from the saturation technique for the three fiber types.

at ~1.53 μm may be calculated. These, together with the gain-loss measurements of Table IV, allow us to determine the peak emission and absorption cross sections. We find them to be as shown in Table VI. These results are presented in Fig. 6(a)–(c).

DISCUSSION

The most important point to note is that the ratios of emission to absorption cross section derived by the two techniques are significantly different (see Tables II and IV). This ratio corresponds to that of maximum gain to loss (where maximum gain is not saturation limited). Since we measured the ratio of gain to loss directly, the Fuchtbauer–Ladenberg approach looks flawed, before even considering the actual values predicted by it for the cross sections.

In applying the Fuchtbauer–Ladenberg analysis, several assumptions are made. The derivation of (8a), relating the cross-section ratio to the absorption and emission linewidths, assumes that the measured spectra are homogeneously broadened. The spectral line shape is dominated by Stark splitting, and this, together with the fast thermal relaxation time between Stark components, results in the system being effectively homogeneously broadened [8], [11] so that this assumption is valid.

A further implicit assumption is that all of the Stark components are equally populated, or the probability of all transitions between the two levels are equal. The first possibility, i.e., equal population, is clearly untrue when we consider that the levels will be populated according to Boltzman statistics [8]. It therefore looks as though the assumption of equal transition probabilities is incorrect—let us therefore look at it in more detail.

The equality of transitions is stated in the Einstein relation

$$B_{12}g_1 = B_{21}g_2; \tag{A6}$$

B_{12} and B_{21} are the probabilities of stimulated absorption and emission, respectively. If we assume a simple two-level model (as indeed we have), then, in the absence of degeneracy, these probabilities would be the same. In the real system, emission and absorption take place between many Stark components and, as we have said above, transitions between the Stark levels of the two bands must have the same probability for the equation to be valid. It is a straightforward matter to test whether the probability of spontaneous transitions between Stark components are identical. By changing the temperature of the fiber, the relative population among the Stark levels is altered. If, as we predict, the transitions have different probabilities, then the fluorescent time constant should be temperature dependent. Results of such measurements made on two of the fibre types are shown in Table VII.

It is quite clear from this information that transitions between different Stark components do indeed have different probabilities; thus, the Fuchtbauer–Ladenberg approach is invalidated in this situation. This result is confirmed by recent work on fluorescence line narrowing [8].

An alternative explanation for the difference obtained for the cross-section ratio by the two techniques would be to invoke a nonradiative decay so that $\tau_{spont} > \tau_{fl}$. The multiphonon decay rate for the $^4I_{13/2} \rightarrow {}^4I_{15/2}$ transition is estimated at $< 1\ s^{-1}$, [12], so that $\tau_{spont} = \tau_{fl}$ is good to 1%, and nonradiative decay is not able to account for the difference in cross-section ratios.

SUMMARY

We have derived emission and absorption cross sections for Er^{3+} doped silica fibers by two independent techniques. The results obtained are significantly at odds with each other. We believe the commonly used spectroscopic technique based on the Fuchtbauer–Ladenberg analysis to be inappropriate, and we have discussed why. Briefly, we find the assumption of equal transition probabilities between Stark components of the two energy levels involved to be incorrect, thus invalidating this approach. With re-

TABLE VII
VARIATION OF FLUORESCENT LIFETIME WITH TEMPERATURE FOR TWO FIBER TYPES

Fiber Type	Temperature		
	77 (K)	300 (K)	800 (K)
GeO_2–SiO_2	15	12	10
Al_2O_3–SiO_2	13	10	9

gard to numerical modeling of Er^{3+} doped fiber-amplifiers and lasers, the data based on saturation measurements presented here should provide a good starting point.

APPENDIX
THE FUCHTBAUER–LADENBERG EQUATIONS

We consider the simple two-level system shown in Fig. 7. The probabilities for spontaneous emission, stimulated emission, and stimulated absorption are A_{21}, B_{21}, and B_{12}. In equilibrium,

$$n_1\rho(\nu)B_{12} = n_2\rho(\nu)B_{21} + n_2A_{21} \tag{A1}$$

where $\rho(\nu)$ is the photon energy density, and n_1 and n_2 are the ground and metastable population densities.

Solving for $\rho(\nu)$,

$$\rho(\nu) = \frac{A_{21}/B_{21}}{B_{12}n_1/B_{21}n_2 - 1}. \tag{A2}$$

By making used of Boltzmann statistics, we can write

$$\frac{n_2}{n_1} = \frac{g_2}{g_1}\exp(h\nu/kT); \tag{A3}$$

substitution into (A5) gives

$$\rho(\nu) = \frac{A_{21}/B_{21}}{g_2B_{12}/g_2B_{21}\exp(h\nu/kT) - 1}. \tag{A4}$$

Now, Planks law can be stated as

$$\rho(\nu)\,d\nu = \frac{8\pi h\nu^3\mu^3}{c^3[\exp(h\nu/kT) - 1]}, \tag{A5}$$

where μ is the refractive index. Combining (A7) and (A8), we find

$$g_1B_{12} = g_2B_{12} \tag{A6}$$

and

$$\frac{A_{21}}{B_{21}} = \frac{8\pi h\nu^3\mu^3}{c_3}. \tag{A7}$$

Now, the stimulated emission rate B_{21} is given by

$$B_{21} = \frac{\sigma_{21}c}{h\nu g(\nu)\mu} \tag{A8}$$

so that

$$\sigma_{21} = \frac{h\nu g(\nu)\mu B_{21}}{c}. \tag{A9}$$

Combining (A10) and (A12), we derive the Fuchtbauer–Ladenberg equation for the emission cross section

$$\sigma_{21} = \frac{\lambda^2}{8\pi\mu^2}A_{21}g(\nu). \tag{A10}$$

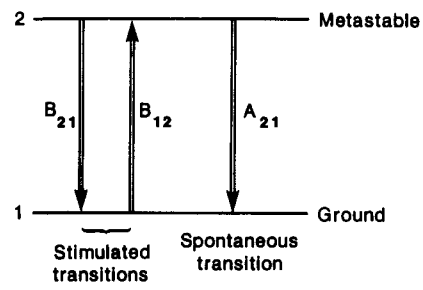

Fig. 7. The two-level system.

If we now consider absorption, we have

$$B_{12} = \frac{\sigma_{12}c}{h\nu g'(\nu)\mu} \tag{A11}$$

where the lineshape for absorption $g'(\nu)$ is not necessarily the same as that for emission $g(\nu)$. The Fuchtbauer–Ladenberg equation for the absorption cross section is thus

$$\sigma_{12} = \frac{g_2}{g_1}\frac{\lambda^2}{8\pi\mu^2}A_{21}g'(\nu). \tag{A12}$$

REFERENCES

[1] R. J. Mears, L. Reekie, I. M. Jauncey, and D. N. Payne, "High gain rare-earth doped fibre amplifier operating at 1.55 μm," in *Proc. OFC*, Reno, NV, 1987, see also, "Low-noise erbium-doped fibre amplifier operating at 1.55 μm," *Electron. Lett.*, vol. 23, pp. 1026–1028, 1987.

[2] E. Desurvire, J. R. Simpson, and P. C. Becker, "High-gain erbium-doped travelling-wave amplifier," *Opt. Lett.*, vol. 12, pp. 888–890, 1987.

[3] M. J. Creaner, D. Spirit, G. R. Walker, N. G. Walker, R. C. Steele, J. Mellis, S. A. Chalabi, W. Hale, I. Sturgess, M. Rutherford, D. Trivett, and M. Brian, "Field demonstation of coherent transmission system with diode pumped erbium-doped fibre amplifiers," *Electron. Lett.*, vol. 26, pp. 442–444, 1990.

[4] J. N. Sandoe and P. H. Sarkies, "Variation of Er^{3+} cross section for stimulated emission with glass composition," *J. Phys. D: Appl. Phys.*, vol. 5, pp. 1788–1799, 1972.

[5] W. J. Miniscalco, L. J. Andrews, B. A. Thompson, T. Wei, and B. T. Hall, "$^4I_{13/2} \Leftrightarrow {}^4I_{15/2}$ emission and absorption cross section for Er^{3+}-doped glasses," in *Proc. OSA, Tunable Solid State Lasers*, 1989.

[6] ——, "The effect of glass composition on the performance of Er^{3+} fibre amplifiers," *SPIE Proc.*, vol. 1171, pp. 93–103, 1989.

[7] C. G. Atkins, J. F. Armitage, R. Wyatt, B. J. Ainslie, and S. P. Criag-Ryan, "High-gain broad spectral bandwidth erbium-doped fibre pumped near 1.5 μm," *Electron. Lett.*, vol. 25, pp. 910–911, 1989.

[8] S. Zemon, G. Lambert, W. J. Miniscalco, L. J. Andrews, and B. T. Hall, "Characterization of Er^{3+} doped glasses by fluorescence line narrowing," *SPIE Proc.*, vol. 1171, pp. 219–236, 1989.

[9] F. Martinez and C. D. Hussey, "(E)ESI determination from mode-field diameter and refractive index profile measurements on single-mode fibres," in *IEEE Proc.*, vol. 135, pp. 202–210, 1988.

[10] M. Artiglia, G. Coppa, P. D. Vita, H. Potenza, and A. Sharma, "Mode field diameter measurements in single mode optical fibres," *J. Lightwave Technol.*, vol. 7, pp. 1139–1152, 1989.

[11] E. Desurvire and J. R. Simpson, "Evaluation of $^4I_{15/2}$ and $^4I_{13/2}$ Stark-level energies in erbium-doped aluminosilicate fibres," in *Opt. Lett.*, vol. 12, pp. 547–549, 1990.

[12] C. B. LAyne, W. H. Lowdermilk, and M. J. Weber, "Nonradiative relaxation of rare-earth ions in silicate laser glass," *IEEE J. Quantum Electron.*, vol. QE-11, pp. 798–799, 1975.

William L. Barnes was born in Haverhill, England, in 1961. He received the B.Sc. and Ph.D. degrees from the University of Exeter in 1983 and 1986, respectively.

In 1986 he joined the Optical Fibre Group, University of Southampton, as a Research Fellow and spent one year working on liquid crystal devices. For the past four years he has been involved in the development of rare-earth-doped fibers for laser and amplifier devices, with particular emphasis on their spectroscopy. In 1989, he became a Senior Research Fellow with the Optoelectronics Research Centre, University of Southampton. He has published nine papers in prestigious international journals and has presented 10 papers (several of which have been Invited) at international conferences throughout the world.

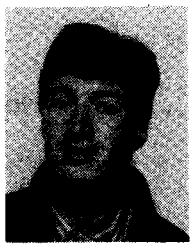

Richard I. Laming was born in Sheffield, England, on March 12, 1962. He received a first class honors degree in mechanical engineering from Nottingham University in 1983 and a Ph.D. degree from Southampton University in 1990.

He was briefly involved with developing engine management systems for the Ford Motor Company Ltd., and in October 1984 he joined the Optical Fibre Group, Southampton University. Since then he has been conducting research on fiber devices which has resulted in over 60 publications and three patents. In 1988 and 1990 he was awarded the Pirelli and Senior Pirelli Research Fellowships, respectively. In October 1990 he was appointed a Royal Society University Research Fellow at the Optoelectronics Centre, Southampton University. His current research interests include erbium-doped fiber amplifiers, mode-locked fiber lasers, and fiber sensors.

Dr. Laming is a Chartered Engineer and member of the Institution of Electrical Engineers. In addition he is the 1989 recipient of the Marconi International Fellowship and Young Scientist of the Year Award.

Eleanor J. Tarbox was born in Surrey, U.K. on August 2, 1953. She received the B.Sc. degree in chemistry and physics in 1974, and the Ph.D. degree in 1977, both from Royal Holloway College, London University. Her doctoral work, supported by British Telecom., involved the study of chemical vapor transport reactions of semiconductor materials used in laser fabrication.

From 1977 to 1979 she was with the BICC Research Laboratories, London, working on optical fiber fabrication. The next five years she spent as a postdoctoral Research Fellow with the Optical Fibre Research Group, Southampton University, designing and fabricating special optical fibers especially high birefringence fiber. Since 1984 she has worked for Pirelli General, U.K., as a Senior Research Engineer in the Optical Systems Group involved in the design and fabrication of special optical fibers, primarily rare earth doped for sensors and optical fiber amplifiers.

P. R. Morkel, photograph and biography not available at the time of publication.